

# A multi-charged particle model with local $U(1)_{\mu-\tau}$ to explain muon $g-2$ , flavor physics, and possible collider signature

Nilanjana Kumar,<sup>1,\*</sup> Takaaki Nomura,<sup>2,†</sup> and Hiroshi Okada<sup>3,4,‡</sup>

<sup>1</sup>*Department of Physics and Astrophysics,  
University of Delhi, Delhi 110007, India*

<sup>2</sup>*School of Physics, KIAS, Seoul 02455, Republic of Korea*

<sup>3</sup>*Asia Pacific Center for Theoretical Physics (APCTP) - Headquarters San 31,  
Hyoja-dong, Nam-gu, Pohang 790-784, Korea*

<sup>4</sup>*Department of Physics, Pohang University of Science  
and Technology, Pohang 37673, Republic of Korea*

(Dated: August 2, 2022)

## Abstract

We consider a model with multi-charged particles including vector-like fermions and a charged scalar under a local  $U(1)_{\mu-\tau}$  symmetry. We search for allowed parameter region explaining muon anomalous magnetic moment (muon  $g-2$ ) and  $b \rightarrow s\ell^+\ell^-$  anomalies, satisfying constraints from the lepton flavor violations,  $Z$  boson decays, meson anti-meson mixing and collider experiments. Carrying out numerical analysis, we explore the typical size of the muon  $g-2$  and Wilson coefficients to explain  $b \rightarrow s\ell^+\ell^-$  anomalies in our model when all other experimental constraints are satisfied. We then discuss the collider physics of the multicharged vectorlike fermions, considering some benchmark points in the allowed parameter space.

---

\*Electronic address: nilanjana.kumar@gmail.com

†Electronic address: nomura@kias.re.kr

‡Electronic address: hiroshi.okada@apctp.org

## I. INTRODUCTION

Muon anomalous magnetic moment (muon  $g - 2$ ) is analyzed with high precision, both experimentally and theoretically and it is a promising observable to test/confirm new physics beyond the standard model(SM). Recently, E989 Run 1 experiment at Fermilab(FNAL) [2] provide new data of muon  $g - 2$  where the previous measurement at the E821 experiment at Brookhaven National Lab (BNL) two decades ago [1] indicates deviation from the SM prediction by  $\sim 3\sigma$ . Combining BNL result, the deviation from the SM prediction [3, 4] is given by

$$\Delta a_\mu = (25.1 \pm 5.9) \times 10^{-10}, \quad (\text{I.1})$$

where the deviation reaches  $4.2\sigma$  with a positive value from the SM prediction. Moreover, further update of Fermilab E989 and upcoming J-PARC E34 [6] experiment will provide the results with higher precision. In order to explain the deviation theoretically, several mechanisms have been proposed historically, for example, gauge contributions [7–9], Yukawa contributions at one-loop level [10], and Barr-Zee contributions [11] at two-loop level. In particular, if muon  $g - 2$  is related to the other phenomenologies such as neutrino mass generations, dark matter and various flavor physics, the new Yukawa interactions become important where muon  $g - 2$  would be explained at one-loop level through such interactions [10, 12–43] (see also recent approaches after new result of FNAL [44–79]). In such case, one has to simultaneously satisfy several constraints of lepton flavor violations (LFVs), such as  $\ell_i \rightarrow \ell_j \gamma$ ,  $\ell_i \rightarrow \ell_j \ell_k \bar{\ell}_\ell$  ( $i, j, k, \ell = (e, \mu, \tau)$ ), and lepton flavor conserving(violating)  $Z$  boson decays  $Z \rightarrow \ell \bar{\ell}'$ ,  $Z \rightarrow \nu \bar{\nu}'$  [80]. In particular,  $\ell_\mu \rightarrow \ell_e \gamma$  process give the most stringent constraint where the current upper bound on the branching ratio is  $4.2 \times 10^{-13}$  [81], and its future bound will reach the sensitivity at  $6 \times 10^{-14}$  [83]. In addition,  $Z$  boson decays will be tested by future experiments such as CEPC [84]. Previously, we analyzed models introducing multi-charged fields (scalars and vector-like leptons) with general  $U(1)_Y$  hypercharges to obtain positive muon  $g - 2$  and explored the parameter region satisfying several experimental constraints [39]. Another interesting study includes a new  $U(1)'$  in order to explain the same [85].

Another interesting hints of new physics are experimental anomalies of semileptonic  $B$ -meson decay; deviations in the measurements of the angular observable  $P'_5$  in the decay of the  $B$  meson ( $B \rightarrow K^* \mu^+ \mu^-$ ) [86–90], the ratio of branching fractions,  $R_K = BR(B^+ \rightarrow$

$K^+\mu^+\mu^-)/BR(B^+ \rightarrow K^+e^+e^-)$  [91–93], and  $R_{K^*} = BR(B \rightarrow K^*\mu^+\mu^-)/BR(B \rightarrow K^*e^+e^-)$  [94]. Various global fits to corresponding Wilson coefficients are also carried out [95–98], indicating that negative contribution to Wilson coefficient associated with  $(\bar{s}_R\gamma^\mu b_L)(\bar{\mu}\gamma_\mu\mu)$  operator is preferred in explaining the anomalies. We can explain the anomalies by introducing  $U(1)_{\mu-\tau}$  gauge symmetry when we include some extra field contents such as vector-like quarks [99–106].

Hence, it is worthwhile to consider a model with multi-charged particles– vector-like quarks, vector-like leptons and charged scalar fields– under local  $U(1)_{\mu-\tau}$  framework where we can combine the ideas in the model discussed in ref. [39] and ref. [99, 104]. Advantages of this scenario are as follows: (1) we can constrain the flavor structure of Yukawa couplings associated with extra fermions in order to suppress the constraints from lepton flavor violations (LFVs), (2) we have more contributions to muon  $g - 2$  from one loop diagrams with  $Z'$  and vector-like leptons, (3) collider signature is controlled by  $U(1)_{\mu-\tau}$  charge assignment to give predictions. We then investigate if both muon  $g - 2$  and  $B$ -anomalies can be explained simultaneously by analyzing the correlation among the parameters taking into account experimental constraints, and discuss collider physics to show possible signatures of this scenario.

In this paper, we discuss the model introducing multi-charged fields (scalars and fermions) under local  $U(1)_{\mu-\tau}$  framework, as an extension of the model in ref. [39] and in ref. [99, 104]. We investigate contributions to muon  $g - 2$  from one-loop diagrams including the new particles such as vector-like lepton, charged scalar and  $Z'$  boson. Extra vector-like quarks are introduced and Wilson coefficient is calculated to explain  $B$ -anomalies. Constraints from meson anti-meson mixing are discussed in addition to LFV and  $Z$  decays. Then we explore the parameter region accommodating both muon  $g - 2$  and  $B$ -anomalies. We search for the parameters satisfying all the constraints and from the allowed model parameters we consider the benchmark points (BP's) for the collider study.

Since the multi-charged fields can be produced at the Large Hadron Collider (LHC), the signature of the exotic charged particles are also explored. We particularly focus on the LHC signatures of exotic lepton doublet. Here the exotic leptons decay *via* the charged scalar, which in turn produces different collider signatures w.r.t the standard scenario, where exotic leptons (singly charged) decay into SM particles directly ( $W\nu$ ,  $Z\ell$  and  $H\ell$ ) [124]. We will show that a small mass difference between the charged scalar and the exotic lepton

	$L_{L\mu}$	$L_{L\tau}$	$e_{R\mu}$	$e_{R\tau}$	$\nu_{R\mu}$	$\nu_{R\tau}$	$L'$	$Q'$	$H$	$s^+$	$\varphi$
$SU(3)$	<b>1</b>	<b>1</b>	<b>1</b>	<b>1</b>	<b>1</b>	<b>1</b>	<b>1</b>	<b>3</b>	<b>1</b>	<b>1</b>	<b>1</b>
$SU(2)_L$	<b>2</b>	<b>2</b>	<b>1</b>	<b>1</b>	<b>1</b>	<b>1</b>	<b>2</b>	<b>2</b>	<b>2</b>	<b>1</b>	<b>1</b>
$U(1)_Y$	$-\frac{1}{2}$	$-\frac{1}{2}$	$-1$	$-1$	$0$	$0$	$-\frac{3}{2}$	$-\frac{5}{6}$	$\frac{1}{2}$	$+1$	$0$
$U(1)_{\mu-\tau}$	$1$	$-1$	$1$	$-1$	$1$	$-1$	$1+x$	$x$	$0$	$-x$	$y$

TABLE I: Charge assignments of fields under  $SU(2)_L \times U(1)_Y \times U(1)_{\mu-\tau}$  for the extended model. We introduce three generations of vector-like fermions  $L'$  and  $Q'$ .

is naturally favored by the sizable muon ( $g-2$ ). Hence, the collider signature of this particular model will contain very soft muons. We particularly focus on the signature of two oppositely charged muon and tau pair at LHC.

This paper is organized as follows. In Sec. II, we show setup of the model and formulate the Wilson coefficient for  $B$ -decay, meson anti-meson mixing, LFV's, muon  $g-2$  and  $Z$  boson decays. In Sec. III, we perform numerical analysis searching for the allowed region of parameter space. In Sec. IV, we discuss possible extension of the model introducing  $U(1)_{\mu-\tau}$  gauge symmetry and discuss collider physics signature. We conclude in Sec. V.

## II. MODEL SETUP AND FORMALISM

We consider a model with gauge symmetry  $G_{\text{SM}} \times U(1)_{\mu-\tau}$  where  $G_{\text{SM}}$  is the SM gauge symmetry and  $U(1)_{\mu-\tau}$  is an extra gauge symmetry. In our set up of the model, we introduce isospin doublet fermions  $L'_a \equiv [\psi_a^-, \psi_a^{--}]^T$  ( $a = 1-3$ ),  $Q'_a \equiv [q_a'^{-1/3}, q_a'^{-4/3}]^T \equiv [u'_a, d'_a]^T$  and a singly-charged boson  $s^+$  as shown in Table I<sup>1</sup>; here  $x$  and  $y$  for  $U(1)_{\mu-\tau}$  are any real number and the SM quarks are not charged under  $U(1)_{\mu-\tau}$ . For vector-like fermions, we introduce three generations to match with the SM. We also introduce three right-handed neutrinos with  $U(1)_{\mu-\tau}$  charge<sup>2</sup> Here, we also introduced scalar field  $\varphi$  with non-zero VEV to break  $U(1)_{\mu-\tau}$  spontaneously. The Lagrangian involving the interaction of new particles and SM

<sup>1</sup> We introduce three generations of vector like fermions just to match with the number of generations for SM fermions. In principle, we can explain anomalies discussed in the paper by one generation of vector like fermion.

<sup>2</sup> In this paper we do not discuss neutrino mass. Neutrino masses under  $U(1)_{\mu-\tau}$  can be found e.g. in ref. [120, 121].

and the potential is given by,

$$\begin{aligned}
-\mathcal{L}_Y^n &= f_{2a} \bar{L}_{L_2} L'_{R_a} s^+ + g_{ia} \bar{Q}_{L_i} Q'_{R_a} s^+ + h_{ij} \bar{L}_{L_i}^c \cdot L_{L_j} s^+ + k_{ij} \overline{\nu_{R_i}^c} e_{R_j} s^+ \\
&\quad + M_{Q'_a} \bar{Q}'_{L_a} Q'_{R_a} + M_{\psi_a} \bar{L}'_{L_a} L'_{R_a} + \text{h.c.} \\
&= f_{2a} [\bar{\nu}_2 P_R \psi_a^- s^+ + \bar{\ell}_2 P_R \psi_a^{--} s^+] + g_{ia} [\bar{u}_i P_R u'_a s^- + \bar{d}_i P_R d'_a s^+] + h_{ij} [\bar{\nu}_i^c P_L \ell_j s^+ - \bar{\ell}_i^c P_L \nu_j s^+] \\
&\quad + k_{ij} \overline{\nu_{R_i}^c} e_{L_j} s^+ + M_{Q'_a} \bar{Q}'_{L_a} Q'_{R_a} + M_{\psi_a} \bar{L}'_{L_a} L'_{R_a} + \text{h.c.}, \tag{II.1}
\end{aligned}$$

$$\begin{aligned}
\mathcal{V} &= \mu_H^2 |H|^2 + \mu_S^2 |s^+|^2 + \lambda_H |H|^4 + \lambda_s |s^+|^4 + \lambda_{Hs} |H|^2 |s^+|^2 + \mu_\varphi^2 |\varphi|^2 + \lambda_\varphi |\varphi|^4 \\
&\quad + \lambda_{H\varphi} |H|^2 |\varphi|^2 + \lambda_{S\varphi} |s^+|^2 |\varphi|^2, \tag{II.2}
\end{aligned}$$

where  $(i, j, a) = 1 - 3$  are generation indices,  $(\cdot \equiv i\sigma_2)$ ,  $\sigma_2$  being the second Pauli matrix, and  $L'_{L[R]_a} (Q'_{L[R]_a}) \equiv P_{L[R]} L'_a (Q'_a)$ . The SM Yukawa term  $y_{\ell_{ii}} \bar{L}_{L_i} e_{R_i} H$  provides masses for the charged leptons ( $m_{\ell_i} \equiv y_{\ell_{ii}} v / \sqrt{2}$ ) by developing a nonzero vacuum expectation value (VEV) of  $H$ , which is denoted by  $\langle H \rangle \equiv v / \sqrt{2}$ . The exotic fermion mass eigenvalues are respectively  $M_{Q'}, M_\psi$  for  $Q', L'$ . We expect that the interaction term involving  $h_{ij}$  plays a role in  $s^+$  decay into the SM fields appropriately. However, since this term gives negative contribution to the muon  $g - 2$ , we assume the scale of  $h_{ij}$  is not so large. It implies that we do not discuss LFVs and muon  $g - 2$  of this term. Note also that non-zero components of  $h_{ij}$  and  $k_{ij}$  are changed by our choice of parameter  $x$ , and thus decay pattern of  $s^+$  depends on  $x$ . More concretely, structure of the third and fourth terms in Eq. (II.1) depends on value of  $x$  such that

$$h_{ij} \bar{L}_{L_i}^c \cdot L_{L_j} s^+ = h_{\{12,13\}} \bar{L}_{L_{\{e,e\}}}^c \cdot L_{L_{\{\mu,\tau\}}} s^+ \quad \text{for } x = \{1, -1\}, \tag{II.3}$$

$$k_{ij} \overline{\nu_{R_i}^c} e_{R_j} s^+ = k_{\{12(21),13(31),22,33\}} \overline{\nu_{R_{\{e(\mu),e(\tau),\mu,\tau\}}}^c} e_{R_{\{\mu(e),\tau(e),\mu,\tau\}}} s^+ \quad \text{for } x = \{1, -1, 2, -2\}, \tag{II.4}$$

where we cannot have the Yukawa interaction for other  $x \neq 0$ . Thus, the decay pattern of  $s^+$  is determined by the choice of  $x$  where we consider our right-handed neutrinos are assumed to be light so that  $s^+$  can decay into states containing them. For  $x = -2$ , constraint from collider experiment is weaker since  $s^\pm$  only decays into third generation of leptons while we have stronger constraint for  $x = \pm 1$  or 2, since it decays into electron and/or muon. Therefore we chose  $x = -2$  in our numerical analysis. In addition we do not have extra term in any choice of  $y$ , where  $x \neq 0$  and  $y \neq 0$ .

In scalar sector, we assume coupling  $\lambda_{H\varphi}$  is small so that mixing between  $\varphi$  and  $H$  is negligible for simplicity. Under the assumption, the VEV of  $\varphi$  is simply given by  $v_\varphi \simeq$

$\sqrt{-\mu_\varphi^2/\lambda_\varphi}$ . After  $\varphi$  developing a VEV, we have massive  $Z'$  boson whose mass is given by

$$m_{Z'} = yg'v_\varphi, \quad (\text{II.5})$$

where  $g'$  is gauge coupling associated with  $U(1)_{\mu-\tau}$ . The mass eigenvalue of  $s^+$  is given by

$$m_S = \mu_S^2 + \frac{\lambda_{Hs}}{2}v^2 + \frac{\lambda_{S\varphi}}{2}v_\varphi^2. \quad (\text{II.6})$$

In our numerical analysis we take  $m_S$  as a free parameter.

### A. $M - \bar{M}$ mixing

The parameter space of our model get constrained from the neutral meson mixings, where the VLQ's appear in the loop. The relevant expressions as shown in [107], are

$$\Delta M_Q \approx \frac{m_Q f_Q^2}{3(4\pi)^2} \sum_{a,b=1}^3 \text{Re}[g_{ka}g_{ai}^*g_{jb}g_{bl}^*] F_{\text{box}}(M_{Q'_a}, M_{Q'_b}, m_s), \quad (\text{II.7})$$

$$F_{\text{box}}(m_1, m_2, m_3) = \int [dx]^3 \frac{z}{xm_1^2 + ym_2^2 + zm_3^2}, \quad (\text{II.8})$$

where  $\int [dx]^3 \equiv \int_0^1 dx dy dz \delta(1-x-y-z)$ ,  $B_s - \bar{B}_s$  mixing corresponds to  $(i, j, k, \ell) = (2, 3, 3, 2)$ ,  $B_d - \bar{B}_d$  mixing corresponds to  $(i, j, k, \ell) = (1, 3, 3, 1)$ ,  $K - \bar{K}$  and  $D - \bar{D}$  to  $(i, j, k, \ell) = (1, 2, 2, 1)$ . The neutral meson mixing formulas should be lower than the experimental bounds as given in [107, 108]:

$$\Delta m_K \lesssim 3.48 \times 10^{-15} \text{ [GeV]}, \quad (\text{II.9})$$

$$3.29 \times 10^{-13} \text{ [GeV]} \lesssim \Delta m_{B_d} + \Delta m_{B_d}^{SM} \lesssim 3.37 \times 10^{-13} \text{ [GeV]}, \quad (\text{II.10})$$

$$1.16 \times 10^{-11} \text{ [GeV]} \lesssim \Delta m_{B_s} + \Delta m_{B_s}^{SM} \lesssim 1.17 \times 10^{-11} \text{ [GeV]}, \quad (\text{II.11})$$

$$\Delta m_D \lesssim 6.25 \times 10^{-15} \text{ [GeV]}, \quad (\text{II.12})$$

where we have taken  $3\sigma$  interval and  $m_M$  and  $f_M$  are the meson mass and the meson decay constant, respectively. The following values of the parameters are used in our analysis:  $f_K \approx 0.156 \text{ GeV}$ ,  $f_{B_d(B_s)} \approx 0.191(0.274) \text{ GeV}$  [109, 110],  $f_D \approx 0.212 \text{ GeV}$ ,  $m_K \approx 0.498 \text{ GeV}$ ,  $m_{B_d(B_s)} \approx 5.280(5.367) \text{ GeV}$ , and  $m_D \approx 1.865 \text{ GeV}$ . The SM contributions are given by [111]:

$$2.96 \times 10^{-13} \text{ [GeV]} \lesssim \Delta m_{B_d}^{SM} \lesssim 5.13 \times 10^{-13} \text{ [GeV]}, \quad (\text{II.13})$$

$$1.06 \times 10^{-11} \text{ [GeV]} \lesssim \Delta m_{B_s}^{SM} \lesssim 1.44 \times 10^{-11} \text{ [GeV]}. \quad (\text{II.14})$$

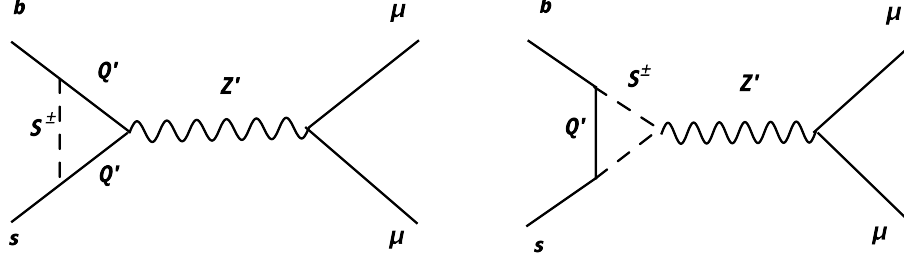


FIG. 1: Diagrams that contributes to  $\Delta C_9^\mu$ .

Subtracting the SM contributions from the experimental results, and one finds the following bounds:

$$-1.85 \times 10^{-13} \text{ [GeV]} \lesssim \Delta m_{B_d} \lesssim 4.05 \times 10^{-14} \text{ [GeV]}, \quad (\text{II.15})$$

$$-2.77 \times 10^{-12} \text{ [GeV]} \lesssim \Delta m_{B_s} \lesssim 1.07 \times 10^{-12} \text{ [GeV]}. \quad (\text{II.16})$$

### B. $b \rightarrow s \ell_i \bar{\ell}_j$ decay

In our model we apply the same mechanism in refs. [99, 104] to generate  $\Delta C_9^\mu$  using  $Z'$  interaction; other mechanisms with  $U(1)_{\mu-\tau}$  can be found in e.g. refs [105, 106]. We obtain contribution to  $\Delta C_9^\mu$  from diagrams in Fig. 1. Then we obtain the contribution to  $\Delta C_9^{\mu, Z'}$  as in Ref [99, 104]

$$\begin{aligned} \Delta C_9^{\mu, Z'} &\simeq \frac{xg'^2}{(4\pi)^2 m_{Z'}^2 C_{\text{SM}}} \sum_{a=1}^3 g_{3a} g_{a2}^* \int [dx]^2 \ln \left( \frac{\Delta[M_{Q'_a}, m_S]}{\Delta[m_S, M_{Q'_a}]} + \frac{M_{Q'_a}^2}{xm_S^2 + yM_{Q'_a}^2} \right), \\ C_{\text{SM}} &\equiv \frac{V_{tb} V_{ts}^* G_F \alpha_{\text{em}}}{\sqrt{2}\pi}, \\ \Delta[m_1, m_2] &= xm_1^2 + ym_2^2, \end{aligned} \quad (\text{II.17})$$

where  $\int [dx]^2 \equiv \int_0^1 dx dy \delta(1-x-y)$  and quark masses are ignored. We can obtain  $\Delta C_9^{\mu, Z'} \sim -1$  satisfying all the experimental constraints as shown in refs. [99, 104] with  $M_{Q'_a} = \mathcal{O}(1)$  TeV,  $m_S = \mathcal{O}(100)$  GeV and  $m_{Z'} = \mathcal{O}(100)$  GeV, where  $Z'$  contribution to muon  $g-2$  is small in this region.

Here, we simplify the above formula by carrying out integration

$$\Delta C_9^{\mu, Z'} \simeq \sum_a \frac{g_{3a} g_{a2}^* x g'^2}{2(4\pi)^2 m_{Z'}^2 C_{\text{SM}}} \quad (\text{II.18})$$

In addition we also obtain Effective Lagrangian to induce  $b \rightarrow s\ell\bar{\ell}$  decay *via* box diagram such that

$$\mathcal{L}^{[\text{box}]} = - \sum_{a,b} \frac{g_{2a}g_{a3}^*f_{2b}f_{b2}^*}{4(4\pi)^2} (\bar{s}\gamma_\mu P_L b)(\bar{\ell}_2\gamma^\mu \ell_2 - \bar{\ell}_2\gamma^\mu \gamma_5 \ell_2) F_{\text{box}}(M_{Q'_a}, M_{\psi_b}, m_s), \quad (\text{II.19})$$

which corresponds to  $\mathcal{O}_9 = -\mathcal{O}_{10}$  [95].

$$\Delta C_9^{\mu[\text{box}]} = -\Delta C_{10}^{\mu[\text{box}]} \approx \sum_{a,b} \frac{g_{2a}g_{a3}^*f_{2b}f_{b2}^*}{4(4\pi)^2 C_{SM}} F_{\text{box}}(M_{Q'_a}, M_{\psi_b}, m_s), \quad (\text{II.20})$$

where  $C_{SM} \equiv \frac{V_{tb}V_{ts}^* G_F \alpha_{em}}{\sqrt{2}\pi}$ . In total, we obtain new physics contribution to the Wilson coefficient,  $\Delta C_9^\ell$ , as

$$\Delta C_9^\mu = \Delta C_9^{\mu, Z'} + \Delta C_9^{\mu[\text{box}]}. \quad (\text{II.21})$$

Furthermore we should take into account the diagrams replacing  $Z'$  by  $Z$  in Fig. 1 which induce flavor universal contributions to  $C_9$  and  $C_{10}$  *via*  $Z$  boson exchange. Calculating the diagrams we obtain

$$\Delta C_9(Z) \simeq \sum_a \frac{g_{3a}g_{a2}^*g_2^2}{4(4\pi)^2 m_Z^2 c_W^2 C_{SM}} \left( -\frac{1}{2} + \frac{4}{3}s_W^2 \right) \left( -\frac{1}{2} + 2s_W^2 \right), \quad (\text{II.22})$$

$$\Delta C_{10}(Z) \simeq \sum_a \frac{g_{3a}g_{a2}^*g_2^2}{8(4\pi)^2 m_Z^2 c_W^2 C_{SM}} \left( -\frac{1}{2} + \frac{4}{3}s_W^2 \right), \quad (\text{II.23})$$

where  $c_W = \cos \theta_W$  with  $\theta_W$  being Weinberg angle. Since structures of  $C_{9,10}(Z)$  are similar to  $\Delta C_9^{\mu, Z'}$  we obtain the relation

$$\frac{\Delta C_9(Z)}{\Delta C_9^{\mu, Z'}} \simeq \frac{g_2^2}{m_Z^2 c_W^2} \frac{m_{Z'}^2}{xg'^2} \frac{1}{2} \left( -\frac{1}{2} + \frac{4}{3}s_W^2 \right) \left( -\frac{1}{2} + 2s_W^2 \right), \quad (\text{II.24})$$

$$\frac{\Delta C_{10}(Z)}{\Delta C_9^{\mu, Z'}} \simeq \frac{g_2^2}{m_Z^2 c_W^2} \frac{m_{Z'}^2}{xg'^2} \frac{1}{4} \left( -\frac{1}{2} + \frac{4}{3}s_W^2 \right). \quad (\text{II.25})$$

Then, the  $b \rightarrow s\mu\bar{\mu}$  anomalies can be explained by  $\Delta C_9^{\mu, Z'} = -0.97$  as the best fit value,  $[-1.12, -0.81]$  at  $1\sigma$ , and  $[-1.27, -0.65]$  at  $2\sigma$  interval [98]. The flavor universal  $\Delta C_9(Z)$  is much smaller than  $\Delta C_9^{\mu, Z'}$  due to the suppression factor  $(-1/2 + 2s_W^2)$ . For  $\Delta C_{10}(Z)$ , we consider constraint from  $B_s \rightarrow \mu^+\mu^-$  measurement. Recent LHCb measurement of the branching ratio is given by [113, 114]

$$BR(B_s^0 \rightarrow \mu^+\mu^-)^{\text{exp}} = (3.09_{-0.43-0.11}^{+0.46+0.15}) \times 10^{-9}, \quad (\text{II.26})$$

where first uncertainty is statical and the second one is systematic. We can estimate the branching ratio in the model such that [115]

$$BR(B_s^0 \rightarrow \mu^+\mu^-)^{\text{th}} = |1 - 0.24\Delta C_{10}^{\mu\mu}|^2 BR(B_s^0 \rightarrow \mu^+\mu^-)^{\text{SM}}, \quad (\text{II.27})$$



where  $BR(B_s^0 \rightarrow \mu^+\mu^-)^{\text{SM}} = (3.65 \pm 0.23) \times 10^{-9}$  is the theoretical predication in the SM [116]. In the numerical analysis we impose that the branching ratio in our model is within  $1\sigma$  region in Eq. (II.26). Note also that  $x < 0$  is preferred since we realize positive  $C_{10}$  to fit the data.

### C. Lepton flavor violations and muon anomalous magnetic moment

In our model we do not have lepton flavor violation from Yukawa coupling  $f_{ia}$  since only components associate with muon,  $f_{2a}$ , are non-zero. We thus only focus on the contribution to muon  $g - 2$  from the Yukawa interactions.

**The muon anomalous magnetic moment ( $\Delta a_\mu$ ):** We can estimate scalar loop contribution to the muon anomalous magnetic moment through(muon  $g - 2$ ), which is given by

$$\Delta a_\mu^S \approx -m_\mu(a_L + a_R)_{22}. \quad (\text{II.28})$$

The amplitude  $a_{L/R}$  can be expressed as,

$$(a_L)_{22} \approx (a_R)_{22} \approx -m_\mu \sum_{a=1-3} \frac{f_{2a}f_{a2}^*}{(4\pi)^2} [F(M_{\psi_a^{--}}, m_S) + 2F(m_S, M_{\psi_a^{--}})], \quad (\text{II.29})$$

where  $M_{\psi^{--}} \equiv M_\psi$ .

It is worthwhile considering  $\Delta a_\mu$  *via*  $Z'$ , even though it would not definitely be needed because we already have the contribution *via*  $f_{2a}$  and preferred mass range is lighter than that for the  $B$  anomalies. The  $Z'$  boson loop contribution is obtained as [117]

$$\Delta a_\mu^{Z'} = \frac{g'^2 m_\mu^2}{4\pi^2} \int_0^1 dx \frac{x^2(1-x)}{x^2 m_\mu^2 + (1-x)m_{Z'}^2}. \quad (\text{II.30})$$

In total muon  $g - 2$  is given by

$$\Delta a_\mu = \Delta a_\mu^S + \Delta a_\mu^{Z'}. \quad (\text{II.31})$$

The measured value show  $3.3\sigma$  deviation from the SM prediction, given by  $\Delta a_\mu = (26.1 \pm 8) \times 10^{-10}$  [3], which is also a positive value. Note here that the charged scalar contribution through  $h_{23}$  is negligible as we consider  $h_{23}$  to be small, as discussed below Eq.(II.2).

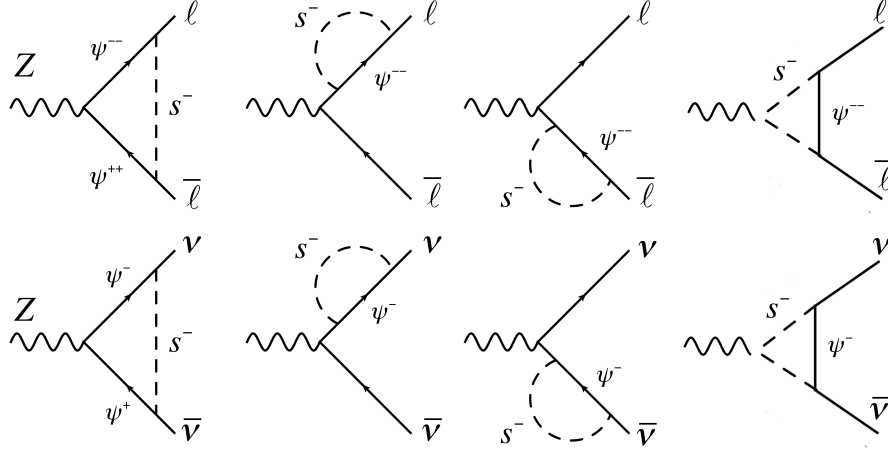


FIG. 2: Feynman diagrams for  $Z \rightarrow \ell_i \bar{\ell}_j$  (up) and  $Z \rightarrow \nu_i \bar{\nu}_j$  (down).

#### D. Flavor-Conserving Leptonic $Z$ Boson Decays

Here, we consider the  $Z$  boson decay into two leptons through the Yukawa terms involving  $f_{2a}$  at one-loop level [26]. Since some components of  $f_{2a}$  are expected to be large in order to obtain the sizable  $\Delta a_\mu$ , the experimental bounds on  $Z$  boson decays could be of concern at one loop level. Note that  $Z$  boson decays are modified only when second generation of leptons are involved due to  $U(1)_{\mu-\tau}$  symmetry. This is why we consider the flavor conserving processes of  $Z$  boson only.

First of all, the relevant Lagrangian is given by <sup>3</sup>

$$\begin{aligned}
\mathcal{L} \sim & \frac{g_2}{c_w} \left[ \bar{\ell} \gamma^\mu \left( -\frac{1}{2} P_L + s_W^2 \right) \ell + \frac{1}{2} \bar{\nu} \gamma^\mu P_L \nu \right] Z_\mu \\
& + \frac{g_2}{c_w} \left[ \left( -\frac{1}{2} P_L + s_W^2 \right) \bar{\psi}^+ \gamma^\mu \psi^- + \left( -\frac{1}{2} P_L + 2s_W^2 \right) \bar{\psi}^{++} \gamma^\mu \psi^{--} \right] Z_\mu \\
& + i \frac{g_2 s_W^2}{c_W} (s^+ \partial^\mu s^- - s^- \partial^\mu s^+) Z_\mu,
\end{aligned} \tag{II.32}$$

where  $s(c)_W \equiv \sin(\cos)\theta_W \sim 0.23$  stands for the sine (cosine) of the Weinberg angle. The

<sup>3</sup> We neglect one-loop contributions in the SM.

decay rate of the SM at tree level is then given by

$$\Gamma(Z \rightarrow \ell_i^- \ell_j^+)_{SM} \approx \frac{m_Z}{12\pi} \frac{g_2^2}{c_W^2} \left( s_W^4 - \frac{s_W^2}{2} + \frac{1}{8} \right) \delta_{ij}, \quad (\text{II.33})$$

$$\Gamma(Z \rightarrow \nu_i \bar{\nu}_j)_{SM} \approx \frac{m_Z}{96\pi} \frac{g_2^2}{c_W^2} \delta_{ij}. \quad (\text{II.34})$$

Combining all the diagrams in Fig. 2, the ultraviolet divergence cancels out and only the finite part remains [26] and is given by,

$$\Delta\Gamma(Z \rightarrow \mu^- \mu^+) \approx \frac{m_Z}{12\pi} \frac{g_2^2}{c_W^2} \left[ \frac{|B_{22}^\ell|^2}{2} - \text{Re}[A_{22}(B^\ell)_{22}^*] - \left( -\frac{s_W^2}{2} + \frac{1}{8} \right) \right], \quad (\text{II.35})$$

$$\Delta\Gamma(Z \rightarrow \nu_\mu \bar{\nu}_\mu) \approx \frac{m_Z}{24\pi} \frac{g_2^2}{c_W^2} \left[ |B_{22}^\nu|^2 - \frac{1}{4} \right], \quad (\text{II.36})$$

where,

$$A_{22} \approx s_W^2, \quad B_{22}^\ell \approx \frac{1}{2} - \sum_a \frac{f_{2a} f_{a2}^\dagger}{(4\pi)^2} G^\ell(M_{\psi_a}, m_S), \quad B_{22}^\nu \approx \frac{1}{2} + \sum_a \frac{f_{2a} f_{a2}^\dagger}{(4\pi)^2} G^\nu(M_{\psi_a}, m_S), \quad (\text{II.37})$$

$$\begin{aligned} G^\ell(M_{\psi_a}, m_S) &\approx -s_W^2 \left( -\frac{1}{2} + s_w^2 \right) H_1(M_{\psi_a}, m_S) - \left( -\frac{1}{2} + s_w^2 \right)^2 H_2(m_{\psi_a}, m_S) \\ &\quad + \left( -\frac{1}{2} + 2s_w^2 \right) H_3(M_{\psi_a}, m_S), \end{aligned} \quad (\text{II.38})$$

$$G^\nu(M_{\psi_a}, m_S) \approx -s_W^2 \left( -\frac{1}{2} + s_w^2 \right) H_1(M_{\psi_a}, m_S) - \frac{1}{2} H_2(M_{\psi_a}, m_S) + \left( -\frac{1}{2} + s_w^2 \right) H_3(M_{\psi_a}, m_S), \quad (\text{II.39})$$

$$H_1(m_1, m_2) = \frac{m_1^4 - m_2^4 + 4m_1^2 m_2^2 \ln \left[ \frac{m_2}{m_1} \right]}{2(m_1^2 - m_2^2)^2}, \quad (\text{II.40})$$

$$H_2(m_1, m_2) = \frac{m_2^4 - 4m_1^2 m_2^2 + 3m_1^4 - 4m_2^2(m_2^2 - 2m_1^2) \ln[m_2] - 4m_1^4 \ln[m_1]}{4(m_1^2 - m_2^2)^2}, \quad (\text{II.41})$$

$$H_3(m_1, m_2) = m_1^2 \left( \frac{m_1^2 - m_2^2 + 2m_2^2 \ln \left[ \frac{m_2}{m_1} \right]}{(m_1^2 - m_2^2)^2} \right). \quad (\text{II.42})$$

Notice here that the upper indices of  $B$  and  $G$ ;  $\ell, \nu$ , respectively represent pairs of the muon and muon-neutrino final states. We consider  $\psi$  as  $\psi^{--}$  inside the argument of  $G^\ell$ , while  $\psi$  as  $\psi^-$  inside the argument of  $G^\nu$ . The current bounds on the lepton-flavor-(conserving)changing  $Z$  boson decay branching ratios at 95 % CL are given by [80]:

$$\Delta\text{BR}(Z \rightarrow \text{Invisible}) \approx \sum_{i,j=1-3} \Delta\text{BR}(Z \rightarrow \nu_i \bar{\nu}_j) < \pm 5.5 \times 10^{-4}, \quad (\text{II.43})$$

$$\Delta\text{BR}(Z \rightarrow \mu^\pm \mu^\mp) < \pm 6.6 \times 10^{-5}, \quad (\text{II.44})$$

where  $\Delta\text{BR}(Z \rightarrow f_i \bar{f}_j)$  ( $i = j$ ) is defined by

$$\Delta\text{BR}(Z \rightarrow f_i \bar{f}_j) \approx \frac{\Gamma(Z \rightarrow f_i \bar{f}_j) - \Gamma(Z \rightarrow f_i \bar{f}_j)_{SM}}{\Gamma_Z^{\text{tot}}}, \quad (\text{II.45})$$

where the total  $Z$  decay width  $\Gamma_Z^{\text{tot}} = 2.4952 \pm 0.0023$  GeV [80]. We consider all these constraints in the numerical analysis in the next section.

### E. Constraints for $Z'$ interaction

Here we discuss experimental constraints for gauge interaction associated with  $Z'$ . The gauge coupling and  $Z'$  mass are restricted by the neutrino trident process  $\nu N \rightarrow \nu N \mu^+ \mu^-$  where  $N$  is a nucleon [7]. The approximated bound is given by  $m_{Z'}/g' \gtrsim 550$  GeV for  $m_{Z'} > 1$  GeV, and we apply the bound in our numerical analysis below.

The gauge interaction is also constrained by the LHC experiment searching for the signal of  $pp \rightarrow \mu^+ \mu^- Z' (\rightarrow \mu^+ \mu^-)$  as given in ref. [119]. The experimental results put the constraint on new gauge coupling in the mass range  $5 \lesssim m_{Z'} \lesssim 70$  GeV. We will compare parameter region explaining  $B$  anomalies with the constraint.

### F. Decay of charged scalar

Finally, we discuss the decay of charged scalar that provides implication to collider physics when we introduce  $U(1)_{\mu-\tau}$  symmetry. As we discussed below Eq. (II.1) charged scalar decays into only third generation of leptons when we chose  $x = -2$ . We then chose  $x = -2$  to relax collider constraint from charged scalar signature. The decay width of  $s^+$  for  $x = -2$  is given by

$$\Gamma_{s^+ \rightarrow \tau_R^\pm \nu_{R\tau}} \simeq \frac{k_{33}^2}{16\pi} m_{S^+}, \quad (\text{II.46})$$

where we ignored lepton mass in the final state assuming light right-handed neutrino. Also we assume right-handed neutrinos are long-lived and it will be just missing energy at collider experiments. Note also that the lightest particle among  $Q'$ ,  $L'$  and  $s^+$  would be stable when there is no interaction associated with  $h_{ij}$  or  $k_{ij}$  in other choices of  $x$  value.

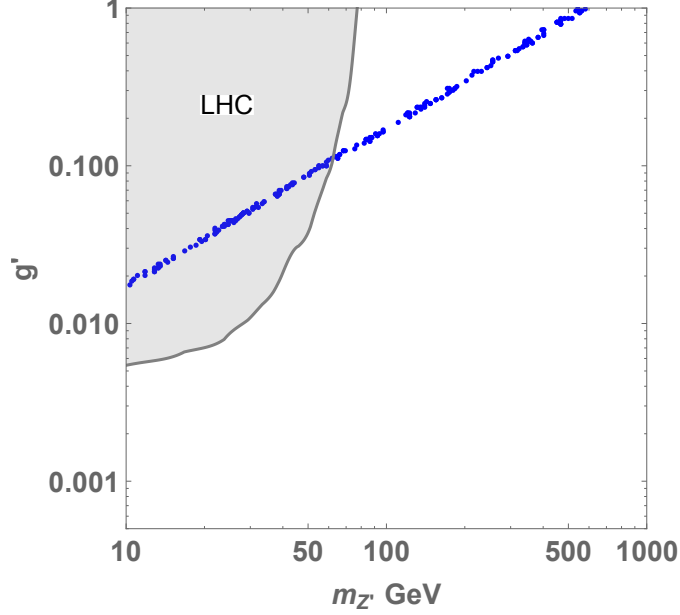


FIG. 3: Allowed points in the parameter space of  $m_{Z'}$  and  $g'$  which can explain the anomaly of  $b \rightarrow s\mu\bar{\mu}$ , providing  $\Delta C_9$  within  $1\sigma$  interval of global fit. We also show the region excluded by  $pp \rightarrow \mu^+\mu^-Z'(\rightarrow \mu^+\mu^-)$  search at the LHC experiment.

### III. NUMERICAL ANALYSIS

In this section we perform a numerical analysis to search for parameter sets which accommodate all the phenomena discussed above. Here we scan our relevant free parameters  $\{g_{ia}, f_{2a}, g', m_{Z'}, M_{\psi_a}, M_{Q_a}, m_S\}$  globally in the following range:

$$\begin{aligned}
g_{ia} &\in [10^{-5}, 1], \quad f_{2a} \in [10^{-2}, 1], \quad g' \in [10^{-3}, 1], \quad m_{Z'} \in [10, 1000] \text{ GeV}, \\
M_{\psi_1} &\in [100, 500] \text{ GeV}, \quad M_{\psi_2} \in [M_{\psi_1}, 750] \text{ GeV}, \quad M_{\psi_3} \in [M_{\psi_2}, 1000] \text{ GeV} \\
M_{Q'_1} &\in [1000, 5000] \text{ GeV}, \quad M_{Q'_2} \in [M_{Q'_1}, 5000] \text{ GeV}, \quad M_{Q'_3} \in [M_{Q'_2}, 5000] \text{ GeV} \\
m_S &\in [M_{\psi_1} - 20, M_{\psi_1} - 10] \text{ GeV},
\end{aligned} \tag{III.1}$$

where we also chose  $x = -2$  for  $U(1)_{\mu-\tau}$  charge assignment. Here we chose values of  $M_{\psi_1}$  and  $m_S$  to be nearly degenerated to avoid constraints from heavy charged lepton search at collider experiments. We find that  $b \rightarrow s\mu\bar{\mu}$  and the neutral meson mixing mainly depends on following Yukawa coupling combinations:

$$C_9^\mu \sim g_{21}g_{13}^*|f_{21}|^2, \quad \Delta m_K \sim g_{21}g_{11}^*, \quad \Delta m_{B_s} \sim g_{31}g_{12}^*, \quad \Delta m_{B_d} \sim g_{31}g_{11}^*, \quad \Delta m_D \sim g_{11}g_{12}^*. \tag{III.2}$$

Since we would like to increase  $C_9^\mu$  as large as possible, while all the meson mixings should be within the experimental ranges, the following hierarchy is preferred

$$g_{11} \ll g_{21} \lesssim g_{31}. \quad (\text{III.3})$$

Then, we estimate  $C_9^\mu$  and muon  $g-2$  imposing experimental constraints. In Fig. 3 we show allowed parameter space in terms of  $m_{Z'}$  and  $g'$  to explain the  $b \rightarrow s\mu\bar{\mu}$  anomalies *via*  $\Delta C_9^{Z'}$  within  $1\sigma$  region of global fit. We also show the parameter region excluded by the LHC measurement searching for  $pp \rightarrow \mu\bar{\mu}Z'(\rightarrow \mu\bar{\mu})$  process [119]. We find that parameter region of  $m_{Z'} \lesssim 50$  GeV is excluded by the LHC constraints while heavier  $Z'$  region can accommodate the  $B$  anomalies. For allowed region, the upper limit of  $g'$  for fixed  $m_{Z'}$  is determined by constraint from neutrino trident while the lower limit is given by constraint from  $BR(B_s^0 \rightarrow \mu^+\mu^-)$ . As a result, we find narrow range of parameter space where region close to neutrino trident limit  $m_{Z'}/g' > 550$  is allowed. Note that the maximum  $|C_9^{\mu[\text{box}]}|$  is 0.115 at most that is out of the  $3\sigma$  range of experimental result due to the stringent constraint arising from  $\Delta m_{B_s}$ , because they ( $\Delta C_9^{\mu[\text{box}]}$  and  $\Delta m_{B_s}$ ) are proportional to the same combination  $g_{31}g_{21}$ .<sup>4</sup> We thus need contribution from  $Z'$  interaction to explain the  $B$  anomalies.

Next we show muon  $g-2$  for allowed parameter sets satisfying all experimental constraints and explaining the  $B$  anomalies. In left(center) plot of Fig. 4, we show contribution to muon  $g-2$  from scalar( $Z'$ ) loop as a function of  $M_{\psi_1}(m_{Z'})$ , and total muon  $g-2$  is shown in the right plot of the figure. We find that contribution from  $Z'$  loop can be larger than  $2 \times 10^{-10}$  for  $m_{Z'} \lesssim 600$  GeV. Notice here that the upper bound up to 600 GeV comes from  $m_{Z'}/g' > 550$  GeV while that above 600 GeV comes from our choice of  $g' < 1$ . The contribution from scalar loop can be larger than  $10^{-10}$  for  $m_{\psi_1} \lesssim 260$  GeV. In particular it can be close to  $10^{-9}$  for  $m_{\psi_1} \sim 100$  GeV region. It is thus possible to explain muon  $g-2$  within  $2\sigma$  level when we add both  $Z'$  and scalar contributions for light  $m_{\psi_1}$  region. We also note that the upper bound on  $f_{21}$  is  $\sim 0.6$  which restrict maximum value of  $\Delta a_\mu^S$ . Here this upper bound of  $f_{21}$  originates from the constraints of  $Z$  boson decays.

---

<sup>4</sup> If one extends  $g_{ai}$  to be complex, then one can evade the constraint of  $\Delta m_{B_s}$  and keep large value of  $|\Delta C_9^\mu|$ . However, in this case, another experimental bound of CP asymmetry  $A_{CP}$  arises and it gives more stringent constraint [112].

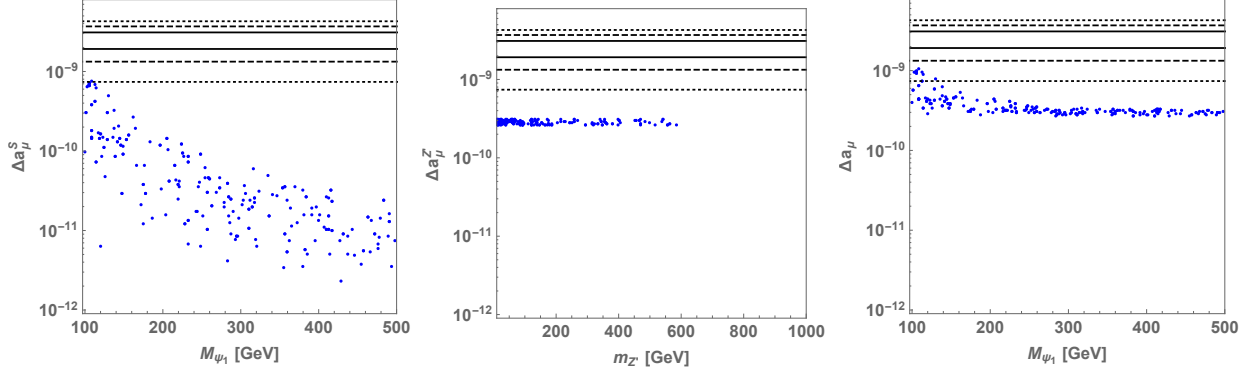


FIG. 4: Left : Contribution to muon  $g - 2$  from scalar loop diagrams. Center : Contribution to muon  $g - 2$  from the  $Z'$  loop diagram. Right: Sum of scalar and  $Z'$  contributions. The regions between solid, dashed and dotted lines indicate  $1 \sigma$ ,  $2 \sigma$  and  $3 \sigma$  region of deviation between observed value and the SM prediction respectively.

### A. Collider physics and constraints

As discussed in the previous subsections, in order to get sizable muon  $g - 2$  satisfying the flavor constraints together, the mass scale (M) of exotic lepton doublet is required to be light; to obtain  $\Delta a_\mu^S \gtrsim \mathcal{O}(10^{-10})$  we need  $M \lesssim 300$  GeV. Here we are interested in the production and decay modes of the doubly charged vector like lepton (VLL) given by,

$$pp \rightarrow \psi^{++}\psi^{--}, \psi^{++} \rightarrow (\mu^+ s^+) \rightarrow \mu^+(\nu_l l^+),$$

$$\psi^{--} \rightarrow (\mu^- s^-) \rightarrow \mu^-(\bar{\nu}_l l^-).$$

Hence the final state is 1 oppositely charged muon pair + 1 oppositely charged lepton ( $l$ ) + MET. As we choose  $f_{21} = 0.5$ ,  $\psi^{\pm\pm}$  will decay mostly in to muon and a charged scalar. Now the coupling of the charged scalar with the SM lepton and the neutrino is defined by  $k_{33}$  as discussed in Sec. II F, and we consider it to be of the order 0.01 where  $s^+$  decays into  $\tau^+ \bar{\nu}_{R\tau}$  with 100 % branching ratio.

Vector like leptons and quarks are constrained from the collider physics experiments. The ATLAS Collaboration performed a search for heavy lepton resonances decaying into a Z boson and a lepton in a multi lepton final state at a center-of-mass energy of 8 TeV [122], constraining singlet VLL model and excluding its mass range of 114–176 GeV. For the doublet VLL model, the L3 Collaboration at LEP placed a lower bound of  $\sim 100$  GeV on

additional heavy leptons [123]. Ref. [124] and [126] have shown that the VLL's in the mass range 120 – 740 GeV are excluded with 95% CL in different multilepton signals. In those analysis, the vectorlike leptons were singly charged and hence it only decays to a SM boson ( $H, W, Z$ ) and SM leptons. While, in our case, VLL's decay in to a charged scalar and muon specifically, followed by the decay of the off-shell or on-shell charged scalar into neutrino and another  $\tau$  lepton. Here we assume  $M_\psi \sim m_S$  and produced muon is less energetic which would be missed at detectors by kinematical cut. Hence the characteristic of our signal is significantly different from Ref. [124] and [126]. Similarly, for vectorlike quarks, the current limit is 1-1.3 TeV [127], but in our model it decays *via* the charged scalar, hence resulting in different final states, not searched so far at LHC.

LEP experiment excludes the charged Higgs masses below 80 GeV [128]. At the LHC, searches for the charged Higgs have been performed through various decay channels,  $H^\pm \rightarrow cs$  [129],  $tb$  [130] and  $\nu\tau^\pm$  [131], and most of these searches exclude  $m_H^\pm < m_t$ . Other searches such as [131] give upper limit on the cross section  $\times$  BR as a function of the charged scalar mass. Notice that  $s^\pm$  only pair produced via  $Z/\gamma$  propagator in  $s$ -channel and the cross section is below the current limit.

In this analysis we choose our selections differently than Ref. [124] and [126]. As a small mass difference between the charged Higgs and the VLL is naturally implied from the muon ( $g - 2$ ), the muon will have a very small  $pT$  ( $\sim 10$ ) GeV, but the other two leptons will have a much higher  $pT$ . Other two leptons are  $\tau$  in our case since we chose  $U(1)_{\mu-\tau}$  charge so that charged scalar couples only  $\tau$  and  $\tau$ -neutrino. This scenario is still allowed for VLL mass  $\leq 300$  GeV. There are scenarios [132, 133] when the doubly charged VLLs decays to a  $W^\pm$  and and lepton( $l^\pm$ ), giving a final state of 2 oppositely charges lepton pair ( $l^\pm$ ) + MET. In this study we have focused on a more exotic scenario, as proposed by the  $U(1)_{\mu-\tau}$  extended model, where the charged exotic leptons decays to tau lepton and a neutrino *via* the charged scalar. Hence in this study we select our signal to be 1 oppositely charged muon pair with very small  $pT$  + 1 oppositely charged tau pair with moderate  $pT$  + MET, and we keep the mass difference between the charged Higgs and the VLL  $\sim 10$  GeV. The same final state has also been studied for a more general model of vector like leptons in Ref. [134]. One of the advantages of VLL with small mass is that the cross section is large which can negate the effect of the suppression due to more than one tau tagging. Moreover, in the VLL signatures studied so far by CMS and ATLAS the assumption was that VLL decays



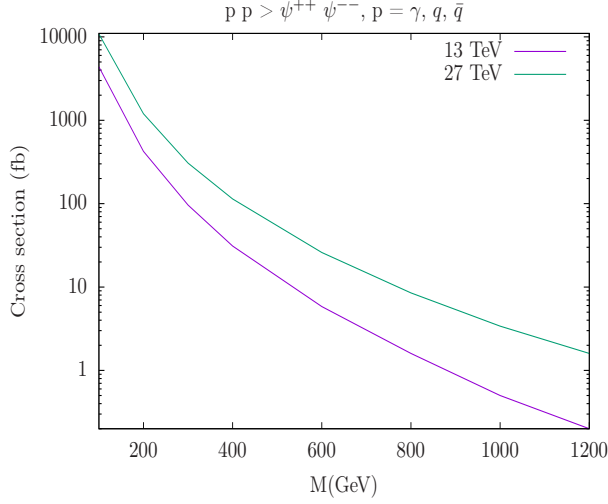


FIG. 5: The cross section for pair production process  $pp \rightarrow \psi^{++}\psi^{--}$  as a function of VLL mass at 13 TeV and 27 TeV.

to a W or Z, which is unlikely in our case. As a result,  $W/Z$  veto can increase the signal efficiency.

We write the model Lagrangian of Eq. (II.1) in FeynRules (v2.3.13) [135, 136]. We generate the model file for MadGraph5\_aMC@NLO (v2.2.1) [137] using FeynRules. Then we calculate the production cross section using the NNPDF23LO1 parton distributions [138] with the factorization and renormalization scales at the central  $m_T^2$  scale after  $k_T$ -clustering of the event. We have computed the signal cross section of  $pp \rightarrow \psi^{++}\psi^{--}$ , where  $p = q, \bar{q}, \gamma$ . The cross sections are normalised to the 5 flavor scheme. The inclusion of the photon PDF increases the signal cross section significantly as the coupling is proportional to the charge of the fermion. We plot the the production cross section in Fig. 5 for 13 TeV as well as 27 TeV <sup>5</sup>. After showering events in PYTHIA [139], events are passed through DELPHES 3 [140] for detector simulation. In DELPHES, we choose the isolation cut for leptons to be  $\Delta R_{max} = 0.5$ , to ensure no hadronic activity inside this isolation cone. While generating the events, we kept the min  $pT$  for muons to be 6 GeV, and also follow other trigger requirements for the soft muons following [141]. The tau tagging efficiency is considered to be 0.6 and the misidentification efficiency is 0.01.

<sup>5</sup> Production cross section  $pp \rightarrow s^+s^-$  is much smaller than that of  $\psi^{++}\psi^{--}$  and mass region  $M(m_S) < 150$  GeV is still allowed by current experimental constraint [131].

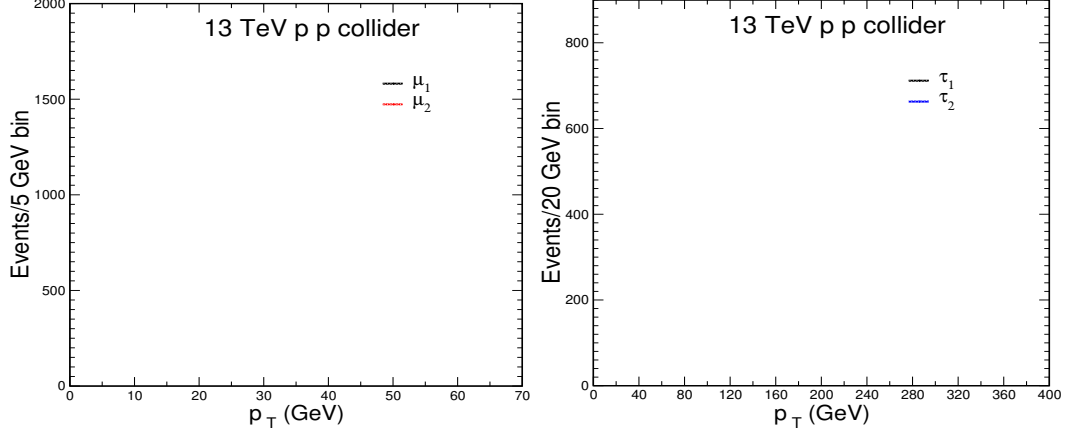


FIG. 6: The transverse momentum distribution of the leading(1) and the subleading(2) muon (left) and tau pairs (right) in unweighted events of  $pp \rightarrow \Psi^{++}\Psi^{--}$  at 13 TeV p-p collision for BP1.

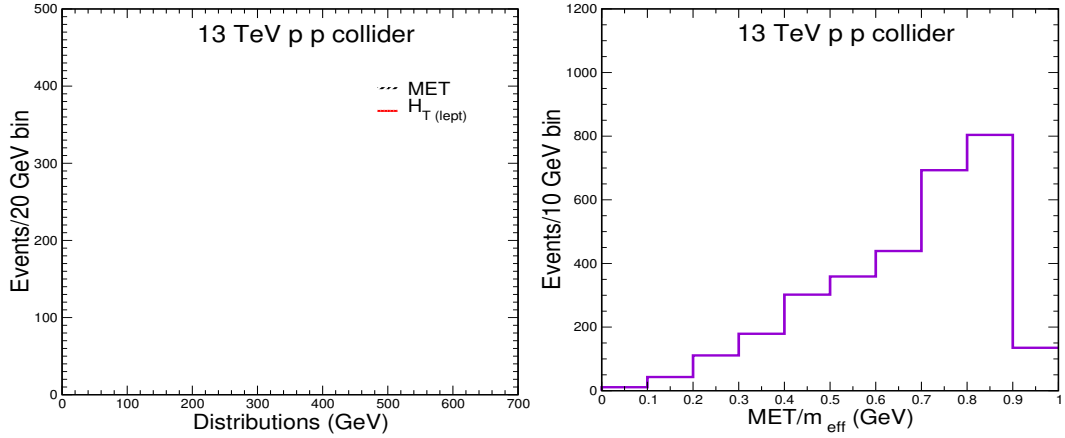


FIG. 7: The transverse missing energy (MET) and sum of all lepton  $p_T$  distribution is shown in the left. In the right the distribution is for the ratio of the MET and  $m_{eff}$ . Events are unweighted and generated by  $pp \rightarrow \Psi^{++}\Psi^{--}$  at 13 TeV p-p collision for BP1.

The  $p_T$  distribution of the leading and subleading tau and muon is shown in Fig. 6 for BP1. In Fig. 7 (left) we show the transverse missing energy and  $H_T(l) = \sum_i p_T(l)_i$  distribution and (right) the ratio  $MET/m_{eff}$  ( $m_{eff} = E_T + H_T(l) + H_T(j)$ ), which is effective to reduce the QCD-jet backgrounds. Based on these distributions we select a set of simple cuts on different kinematic variables.

### Selection 1:

- Opposite sign same flavor pair of mu and tau  $(\mu^+\mu^-) + (\tau^+\tau^-)$ ,
- $p_T(\mu_1) > 6 \text{ GeV}$ ,  $p_T(\mu_2) > 6 \text{ GeV}$ ,  $p_T(\tau_1) > 60 \text{ GeV}$ ,  $p_T(\tau_2) > 40 \text{ GeV}$ ,
- $|\eta(\mu, \tau)| < 2.5$ ,  $\Delta R(l, l) > 0.3$ ,

**Selection2:**

- b-jet veto,  $MET > 100 \text{ GeV}$ ,  $H_T > 150 \text{ GeV}$ ,
- $MET/m_{eff} > 0.5$ ,

**Selection3:**

- Z veto with  $M_Z \pm 10 \text{ GeV}$ .

We show the signal cross section after the selections in Table. II for three BP's. One can see that for this multilepton channel the cross section is well above 1 fb after the selections. The signal does not suffer much from the Z-veto which is a big advantage for our signal as Z veto is effective to reduce the backgrounds from Z decays. b-jet veto and the requirement of higher ratio of MET and  $m_{eff}$  will also be effective to reduce the background for these type of signal. For the discussion on the background of this particular channel one can see Ref. [134]. In general multilepton channel possesses less background compared to the other processes. After Selection3, the number of events at  $150 \text{ fb}^{-1}$  is always more than 150 if background is very small, which makes this channel a good candidate look for new physics at 13 TeV LHC run.

## IV. CONCLUSION

We have analyzed muon (g-2), LFVs, Z decays,  $\Delta C_9^\mu$  for B-anomalies, and  $M-\bar{M}$  mixing in a framework of multi-charged particles which includes exotic scalars, leptons and quarks under the local  $U(1)_{\mu-\tau}$ . Thanks to the gauge symmetry we can suppress the LFV process which could appear from Yukawa interactions among exotic lepton, charged scalar and the SM lepton. As a result, we found that the sizable Yukawa couplings are naturally allowed to explain muon  $g - 2$ . We have first formulated phenomenological observables mentioned above in our model and performed numerical analysis to search for allowed parameter sets.

-	BP1	BP2	BP3
$k_{33} = 0.01$	$g_{31} \approx -0.368, M_{Q'} = 1083$	$g_{31} \approx 0.32, M_{Q'} = 1200$	$g_{31} \approx -0.1080, M_{Q'} = 1201$
	$g_{21} \approx 0.166, m_s \approx 272$	$g_{21} \approx 0.2060, m_s \approx 230$	$g_{21} \approx -0.6240, m_s \approx 304$
	$g_{11} \approx -0.0468, M \approx 284$	$g_{11} \approx -0.0014, M \approx 250$	$g_{11} \approx 0.0071, M \approx 320$
Selection 1	3.44 ( <i>9.58</i> ) fb	2.87 ( <i>11.06</i> ) fb	2.67 ( <i>9.62</i> ) fb
Selection 2	1.76 ( <i>7.31</i> ) fb	1.22 ( <i>4.88</i> ) fb	1.49 ( <i>4.36</i> ) fb
Selection 3	1.63 ( <i>5.82</i> ) fb	1.06 ( <i>3.28</i> ) fb	1.38 ( <i>4.96</i> ) fb

TABLE II: Signal cross section (fb) after the selections at three different benchmark points at 13 TeV and 27 TeV (italic). Masses are in GeV.

Carrying out numerical calculations, we have found that our  $\Delta C_9^\mu$  can accommodate  $B$ -anomalies where  $Z'$  boson contribution is dominant. On the other hand, contribution from box diagram in  $\Delta C_9^{\mu[\text{box}]}$  can only reach the value  $\sim -0.1$  when we impose constraints from  $Z \rightarrow \nu_i \bar{\nu}_j$  invisible decay,  $Z \rightarrow \mu \bar{\mu}$  decay and  $B_s - \bar{B}_s$  mixing. This is due to the stringent constraints from  $B_s - \bar{B}_s$  mixing and  $Z \rightarrow \mu \bar{\mu}$  which restrict the relevant Yukawa coupling constants. We have shown that the muon  $g - 2$  in our model is sum of the contributions from scalar boson loop and  $Z'$  loop diagrams. It has been found that we can explain muon  $g - 2$  within  $2\sigma$  level when we include both these contributions. Finally, we have studied the collider physics focusing on the production of doubly charged leptons using some benchmark points allowed by the numerical analysis. We have shown that the channel with pairs of oppositely charged muon and tau has some unique features that distinguish our model signatures from other vector like lepton signatures at LHC. The exotic vector like quarks and the  $Z'$  will also give interesting collider phenomenology but we keep that for future study.

## Acknowledgments

This research was supported by an appointment to the JRG Program at the APCTP through the Science and Technology Promotion Fund and Lottery Fund of the Korean Government. This was also supported by the Korean Local Governments - Gyeongsangbuk-do Province and Pohang City (H.O.). H. O. is sincerely grateful for the KIAS member, and log

cabin at POSTECH to provide nice space to come up with this project. N.K. acknowledges the support from the Dr. D. S. Kothari Postdoctoral scheme (201819-PH/18-19/0013). N. K. also acknowledges “(9/27-28 @APCTP HQ) APCTP Mini-Workshop - Recent topics on dark matter, neutrino, and their related phenomenologies” where the problem was proposed and also thanks the hospitality of APCTP, Korea.

- 
- [1] G. W. Bennett *et al.* [Muon g-2], Phys. Rev. D **73**, 072003 (2006) [arXiv:hep-ex/0602035 [hep-ex]].
  - [2] B. Abi *et al.* [Muon g-2], Phys. Rev. Lett. **126**, 141801 (2021) [arXiv:2104.03281 [hep-ex]].
  - [3] K. Hagiwara, R. Liao, A. D. Martin, D. Nomura and T. Teubner, J. Phys. G **38**, 085003 (2011) [arXiv:1105.3149 [hep-ph]].
  - [4] A. Keshavarzi, D. Nomura and T. Teubner, Phys. Rev. D **97**, no. 11, 114025 (2018) [arXiv:1802.02995 [hep-ph]].
  - [5] J. Grange *et al.* (Muon g-2) (2015), 1501.06858.
  - [6] H. Inuma (J-PARC muon g-2/EDM), J. Phys. Conf. Ser. 295, 012032 (2011).
  - [7] W. Altmannshofer, S. Gori, M. Pospelov and I. Yavin, Phys. Rev. Lett. **113**, 091801 (2014) [arXiv:1406.2332 [hep-ph]].
  - [8] G. Mohlabeng, arXiv:1902.05075 [hep-ph].
  - [9] W. Abdallah, A. Awad, S. Khalil and H. Okada, Eur. Phys. J. C **72**, 2108 (2012) [arXiv:1105.1047 [hep-ph]].
  - [10] M. Lindner, M. Platscher and F. S. Queiroz, Phys. Rept. **731**, 1 (2018) [arXiv:1610.06587 [hep-ph]].
  - [11] S. M. Barr and A. Zee, Phys. Rev. Lett. 65 (1990) 21 [Erratum-ibid. 65 (1990) 2920].
  - [12] A. E. Cárcamo Hernández, S. Kovalenko, R. Pasechnik and I. Schmidt, arXiv:1901.09552 [hep-ph].
  - [13] E. Ma and M. Raidal, Phys. Rev. Lett. **87**, 011802 (2001) Erratum: [Phys. Rev. Lett. **87**, 159901 (2001)] [hep-ph/0102255].
  - [14] H. Okada and K. Yagyu, Phys. Rev. D **89**, no. 5, 053008 (2014) [arXiv:1311.4360 [hep-ph]].
  - [15] S. Baek, H. Okada and T. Toma, Phys. Lett. B **732**, 85 (2014) [arXiv:1401.6921 [hep-ph]].
  - [16] H. Okada and K. Yagyu, Phys. Rev. D **90**, no. 3, 035019 (2014) [arXiv:1405.2368 [hep-ph]].

- [17] H. Okada, T. Toma and K. Yagyu, Phys. Rev. D **90**, 095005 (2014) [arXiv:1408.0961 [hep-ph]].
- [18] H. Okada and K. Yagyu, Phys. Rev. D **93**, no. 1, 013004 (2016) [arXiv:1508.01046 [hep-ph]].
- [19] H. Okada and K. Yagyu, Phys. Lett. B **756**, 337 (2016) [arXiv:1601.05038 [hep-ph]].
- [20] T. Nomura and H. Okada, Phys. Lett. B **756**, 295 (2016) [arXiv:1601.07339 [hep-ph]].
- [21] P. Ko, T. Nomura, H. Okada and Y. Orikasa, Phys. Rev. D **94**, no. 1, 013009 (2016) [arXiv:1602.07214 [hep-ph]].
- [22] S. Baek, T. Nomura and H. Okada, Phys. Lett. B **759**, 91 (2016) [arXiv:1604.03738 [hep-ph]].
- [23] W. Altmannshofer, M. Carena and A. Crivellin, Phys. Rev. D **94**, no. 9, 095026 (2016) [arXiv:1604.08221 [hep-ph]].
- [24] T. Nomura and H. Okada, Phys. Rev. D **94**, 075021 (2016) [arXiv:1607.04952 [hep-ph]].
- [25] S. Lee, T. Nomura and H. Okada, Nucl. Phys. B **931**, 179 (2018) [arXiv:1702.03733 [hep-ph]].
- [26] C. W. Chiang, H. Okada and E. Senaha, Phys. Rev. D **96**, no. 1, 015002 (2017) [arXiv:1703.09153 [hep-ph]].
- [27] A. Das, T. Nomura, H. Okada and S. Roy, Phys. Rev. D **96**, no. 7, 075001 (2017) [arXiv:1704.02078 [hep-ph]].
- [28] T. Nomura and H. Okada, Phys. Rev. D **96**, no. 1, 015016 (2017) [arXiv:1704.03382 [hep-ph]].
- [29] T. Nomura and H. Okada, Int. J. Mod. Phys. A **33**, no. 14n15, 1850089 (2018) [arXiv:1706.05268 [hep-ph]].
- [30] K. Cheung and H. Okada, Phys. Lett. B **774**, 446 (2017) [arXiv:1708.06111 [hep-ph]].
- [31] K. Cheung and H. Okada, Phys. Rev. D **97**, no. 7, 075027 (2018) [arXiv:1801.00585 [hep-ph]].
- [32] Y. Cai, J. Herrero-García, M. A. Schmidt, A. Vicente and R. R. Volkas, Front. in Phys. **5**, 63 (2017) [arXiv:1706.08524 [hep-ph]].
- [33] T. Nomura and H. Okada, Phys. Dark Univ. **21**, 90 (2018) [arXiv:1712.00941 [hep-ph]].
- [34] S. Baumholzer, V. Brdar and P. Schwaller, JHEP **1808**, 067 (2018) [arXiv:1806.06864 [hep-ph]].
- [35] N. Chakrabarty, C. W. Chiang, T. Ohata and K. Tsumura, JHEP **1812**, 104 (2018) [arXiv:1807.08167 [hep-ph]].
- [36] B. Barman, D. Borah, L. Mukherjee and S. Nandi, Phys. Rev. D **100**, no. 11, 115010 (2019) [arXiv:1808.06639 [hep-ph]].
- [37] C. H. Chen and T. Nomura, arXiv:1903.03380 [hep-ph].

- [38] P. Arnan, A. Crivellin, M. Fedele and F. Mescia, JHEP **1906**, 118 (2019) [arXiv:1904.05890 [hep-ph]].
- [39] T. Nomura and H. Okada, Phys. Rev. D **101**, no. 1, 015021 (2020) [arXiv:1903.05958 [hep-ph]].
- [40] S. P. Li and X. Q. Li, arXiv:1907.13555 [hep-ph].
- [41] L. Calibbi, T. Li, Y. Li and B. Zhu, arXiv:1912.02676 [hep-ph].
- [42] C. H. Chen and T. Nomura, arXiv:2001.07515 [hep-ph].
- [43] L. Darmé, M. Fedele, K. Kowalska and E. M. Sessolo, arXiv:2002.11150 [hep-ph].
- [44] G. Arcadi, L. Calibbi, M. Fedele and F. Mescia, Phys. Rev. Lett. **127**, no.6, 061802 (2021) [arXiv:2104.03228 [hep-ph]].
- [45] B. Zhu and X. Liu, [arXiv:2104.03238 [hep-ph]].
- [46] X. F. Han, T. Li, H. X. Wang, L. Wang and Y. Zhang, [arXiv:2104.03227 [hep-ph]].
- [47] S. Baum, M. Carena, N. R. Shah and C. E. M. Wagner, [arXiv:2104.03302 [hep-ph]].
- [48] Y. Bai and J. Berger, [arXiv:2104.03301 [hep-ph]].
- [49] P. Das, M. K. Das and N. Khan, [arXiv:2104.03271 [hep-ph]].
- [50] C. T. Lu, R. Ramos and Y. L. S. Tsai, doi:10.1007/JHEP08(2021)073 [arXiv:2104.04503 [hep-ph]].
- [51] S. F. Ge, X. D. Ma and P. Pasquini, Eur. Phys. J. C **81**, no.9, 787 (2021) doi:10.1140/epjc/s10052-021-09571-1 [arXiv:2104.03276 [hep-ph]].
- [52] V. Brdar, S. Jana, J. Kubo and M. Lindner, Phys. Lett. B **820**, 136529 (2021) doi:10.1016/j.physletb.2021.136529 [arXiv:2104.03282 [hep-ph]].
- [53] M. A. Buen-Abad, J. Fan, M. Reece and C. Sun, JHEP **09**, 101 (2021) doi:10.1007/JHEP09(2021)101 [arXiv:2104.03267 [hep-ph]].
- [54] L. Zu, X. Pan, L. Feng, Q. Yuan and Y. Z. Fan, [arXiv:2104.03340 [hep-ph]].
- [55] D. W. P. Amaral, D. G. Cerdeno, A. Cheek and P. Foldenauer, Eur. Phys. J. C **81**, 861 (2021) doi:10.1140/epjc/s10052-021-09670-z [arXiv:2104.03297 [hep-ph]].
- [56] M. Endo, K. Hamaguchi, S. Iwamoto and T. Kitahara, JHEP **07**, 075 (2021) doi:10.1007/JHEP07(2021)075 [arXiv:2104.03217 [hep-ph]].
- [57] W. Ahmed, I. Khan, J. Li, T. Li, S. Raza and W. Zhang, [arXiv:2104.03491 [hep-ph]].
- [58] M. Abdughani, Y. Z. Fan, L. Feng, Y. L. S. Tsai, L. Wu and Q. Yuan, Sci. Bull. **66**, 2170-2174 (2021) doi:10.1016/j.scib.2021.07.029 [arXiv:2104.03274 [hep-ph]].

- [59] M. Van Beekveld, W. Beenakker, M. Schutten and J. De Wit, SciPost Phys. **11**, no.3, 049 (2021) doi:10.21468/SciPostPhys.11.3.049 [arXiv:2104.03245 [hep-ph]].
- [60] P. Cox, C. Han and T. T. Yanagida, [arXiv:2104.03290 [hep-ph]].
- [61] F. Wang, L. Wu, Y. Xiao, J. M. Yang and Y. Zhang, Nucl. Phys. B **970**, 115486 (2021) doi:10.1016/j.nuclphysb.2021.115486 [arXiv:2104.03262 [hep-ph]].
- [62] Y. Gu, N. Liu, L. Su and D. Wang, Nucl. Phys. B **969**, 115481 (2021) doi:10.1016/j.nuclphysb.2021.115481 [arXiv:2104.03239 [hep-ph]].
- [63] J. Cao, J. Lian, Y. Pan, D. Zhang and P. Zhu, JHEP **09**, 175 (2021) doi:10.1007/JHEP09(2021)175 [arXiv:2104.03284 [hep-ph]].
- [64] W. Yin, JHEP **06**, 029 (2021) doi:10.1007/JHEP06(2021)029 [arXiv:2104.03259 [hep-ph]].
- [65] C. Han, [arXiv:2104.03292 [hep-ph]].
- [66] A. Aboubrahim, M. Klasen and P. Nath, Phys. Rev. D **104**, no.3, 035039 (2021) doi:10.1103/PhysRevD.104.035039 [arXiv:2104.03839 [hep-ph]].
- [67] J. L. Yang, H. B. Zhang, C. X. Liu, X. X. Dong and T. F. Feng, doi:10.1007/JHEP08(2021)086 [arXiv:2104.03542 [hep-ph]].
- [68] M. Chakraborti, L. Roszkowski and S. Trojanowski, JHEP **05**, 252 (2021) doi:10.1007/JHEP05(2021)252 [arXiv:2104.04458 [hep-ph]].
- [69] P. M. Ferreira, B. L. Gonçalves, F. R. Joaquim and M. Sher, Phys. Rev. D **104**, no.5, 053008 (2021) doi:10.1103/PhysRevD.104.053008 [arXiv:2104.03367 [hep-ph]].
- [70] H. X. Wang, L. Wang and Y. Zhang, [arXiv:2104.03242 [hep-ph]].
- [71] T. Li, J. Pei and W. Zhang, doi:10.1140/epjc/s10052-021-09474-1 [arXiv:2104.03334 [hep-ph]].
- [72] M. Cadeddu, N. Cargioli, F. Dordei, C. Giunti and E. Picciau, Phys. Rev. D **104**, no.1, 011701 (2021) doi:10.1103/PhysRevD.104.L011701 [arXiv:2104.03280 [hep-ph]].
- [73] L. Calibbi, M. L. López-Ibañez, A. Melis and O. Vives, Eur. Phys. J. C **81**, no.10, 929 (2021) doi:10.1140/epjc/s10052-021-09741-1 [arXiv:2104.03296 [hep-ph]].
- [74] J. Chen, Q. Wen, F. Xu and M. Zhang, [arXiv:2104.03699 [hep-ph]].
- [75] P. Escribano, J. Terol-Calvo and A. Vicente, Phys. Rev. D **103**, no.11, 115018 (2021) doi:10.1103/PhysRevD.103.115018 [arXiv:2104.03705 [hep-ph]].
- [76] J. C. Eung and T. Mondal, JHEP **07**, 044 (2021) doi:10.1007/JHEP07(2021)044 [arXiv:2104.03701 [hep-ph]].



- [77] G. Arcadi, Á. S. De Jesus, T. B. De Melo, F. S. Queiroz and Y. S. Villamizar, [arXiv:2104.04456 [hep-ph]].
- [78] C. H. Chen, C. W. Chiang and T. Nomura, Phys. Rev. D **104**, no.5, 055011 (2021) doi:10.1103/PhysRevD.104.055011 [arXiv:2104.03275 [hep-ph]].
- [79] T. Nomura and H. Okada, Phys. Rev. D **104**, no.3, 035042 (2021) doi:10.1103/PhysRevD.104.035042 [arXiv:2104.03248 [hep-ph]].
- [80] M. Tanabashi *et al.* [Particle Data Group], Phys. Rev. D **98**, no. 3, 030001 (2018).
- [81] A. M. Baldini *et al.* [MEG Collaboration], Eur. Phys. J. C **76**, no. 8, 434 (2016) [arXiv:1605.05081 [hep-ex]].
- [82] B. Aubert *et al.* [BaBar Collaboration], Phys. Rev. Lett. **104** (2010) 021802 [arXiv:0908.2381 [hep-ex]].
- [83] F. Renga [MEG Collaboration], Hyperfine Interact. **239**, no. 1, 58 (2018) [arXiv:1811.05921 [hep-ex]].
- [84] CEPC-SPPC Study Group, IHEP-CEPC-DR-2015-01, IHEP-TH-2015-01, IHEP-EP-2015-01.
- [85] J. Kawamura, S. Raby and A. Trautner, Phys. Rev. D **100**, no.5, 055030 (2019) doi:10.1103/PhysRevD.100.055030 [arXiv:1906.11297 [hep-ph]].
- [86] S. Descotes-Genon, J. Matias, M. Ramon and J. Virto, JHEP **1301**, 048 (2013) [arXiv:1207.2753 [hep-ph]].
- [87] R. Aaij *et al.* [LHCb Collaboration], JHEP **1602**, 104 (2016) [arXiv:1512.04442 [hep-ex]].
- [88] R. Aaij *et al.* [LHCb Collaboration], Phys. Rev. Lett. **111**, 191801 (2013) [arXiv:1308.1707 [hep-ex]].
- [89] A. Abdesselam *et al.* [Belle Collaboration], arXiv:1604.04042 [hep-ex].
- [90] S. Wehle *et al.* [Belle Collaboration], arXiv:1612.05014 [hep-ex].
- [91] G. Hiller and F. Kruger, Phys. Rev. D **69**, 074020 (2004) [hep-ph/0310219].
- [92] C. Bobeth, G. Hiller and G. Piranishvili, JHEP **0712**, 040 (2007) [arXiv:0709.4174 [hep-ph]].
- [93] R. Aaij *et al.* [LHCb Collaboration], Phys. Rev. Lett. **113**, 151601 (2014) [arXiv:1406.6482 [hep-ex]].
- [94] R. Aaij *et al.* [LHCb Collaboration], arXiv:1705.05802 [hep-ex].
- [95] S. Descotes-Genon, L. Hofer, J. Matias and J. Virto, JHEP **1606**, 092 (2016) [arXiv:1510.04239 [hep-ph]].

- [96] M. Ciuchini, A. M. Coutinho, M. Fedele, E. Franco, A. Paul, L. Silvestrini and M. Valli, Eur. Phys. J. C **79**, no. 8, 719 (2019) [arXiv:1903.09632 [hep-ph]].
- [97] M. Algueró, B. Capdevila, A. Crivellin, S. Descotes-Genon, P. Masjuan, J. Matias and J. Virto, Eur. Phys. J. C **79**, no. 8, 714 (2019) [arXiv:1903.09578 [hep-ph]].
- [98] J. Aebischer, W. Altmannshofer, D. Guadagnoli, M. Reboud, P. Stangl and D. M. Straub, arXiv:1903.10434 [hep-ph].
- [99] P. Ko, T. Nomura and H. Okada, Phys. Rev. D **95**, no. 11, 111701 (2017) [arXiv:1702.02699 [hep-ph]].
- [100] W. Altmannshofer and I. Yavin, Phys. Rev. D **92** (2015) no.7, 075022 [arXiv:1508.07009 [hep-ph]].
- [101] W. Altmannshofer, S. Gori, S. Profumo and F. S. Queiroz, JHEP **12** (2016), 106 [arXiv:1609.04026 [hep-ph]].
- [102] C. H. Chen and T. Nomura, Phys. Lett. B **777** (2018), 420-427 [arXiv:1707.03249 [hep-ph]].
- [103] G. Arcadi, T. Hugle and F. S. Queiroz, Phys. Lett. B **784** (2018), 151-158 [arXiv:1803.05723 [hep-ph]].
- [104] P. T. P. Hutaauruk, T. Nomura, H. Okada and Y. Orikasa, Phys. Rev. D **99**, no. 5, 055041 (2019) [arXiv:1901.03932 [hep-ph]].
- [105] W. Altmannshofer, S. Gori, M. Pospelov and I. Yavin, Phys. Rev. D **89**, 095033 (2014) [arXiv:1403.1269 [hep-ph]].
- [106] A. Crivellin, G. D'Ambrosio and J. Heeck, Phys. Rev. Lett. **114**, 151801 (2015) [arXiv:1501.00993 [hep-ph]].
- [107] F. Gabbiani, E. Gabrielli, A. Masiero and L. Silvestrini, Nucl. Phys. B **477**, 321 (1996) [hep-ph/9604387].
- [108] K. A. Olive *et al.* [Particle Data Group], Chin. Phys. C **38**, 090001 (2014).
- [109] L. Di Luzio, M. Kirk and A. Lenz, Phys. Rev. D **97**, no. 9, 095035 (2018) [arXiv:1712.06572 [hep-ph]].
- [110] L. Di Luzio, M. Kirk and A. Lenz, arXiv:1811.12884 [hep-ph].
- [111] Y. Amhis *et al.* [HFLAV Collaboration], Eur. Phys. J. C **77**, no. 12, 895 (2017) [arXiv:1612.07233 [hep-ex]].
- [112] L. Di Luzio, M. Kirk, A. Lenz and T. Rauh, JHEP **1912**, 009 (2019) [arXiv:1909.11087 [hep-ph]].

- [113] R. Aaij *et al.* [LHCb], [arXiv:2108.09283 [hep-ex]].
- [114] R. Aaij *et al.* [LHCb], [arXiv:2108.09284 [hep-ex]].
- [115] G. Hiller and M. Schmaltz, Phys. Rev. D **90**, 054014 (2014) doi:10.1103/PhysRevD.90.054014 [arXiv:1408.1627 [hep-ph]].
- [116] C. Bobeth, M. Gorbahn, T. Hermann, M. Misiak, E. Stamou and M. Steinhauser, Phys. Rev. Lett. **112**, 101801 (2014) doi:10.1103/PhysRevLett.112.101801 [arXiv:1311.0903 [hep-ph]].
- [117] T. Nomura and H. Okada, Phys. Lett. B **783**, 381 (2018) [arXiv:1805.03942 [hep-ph]].
- [118] S. R. Mishra *et al.* [CCFR Collaboration], Phys. Rev. Lett. **66**, 3117 (1991).
- [119] A. M. Sirunyan *et al.* [CMS Collaboration], Phys. Lett. B **792**, 345 (2019) [arXiv:1808.03684 [hep-ex]].
- [120] K. Asai, K. Hamaguchi and N. Nagata, Eur. Phys. J. C **77**, no.11, 763 (2017) [arXiv:1705.00419 [hep-ph]].
- [121] K. Asai, K. Hamaguchi, N. Nagata, S. Y. Tseng and K. Tsumura, Phys. Rev. D **99**, no.5, 055029 (2019) [arXiv:1811.07571 [hep-ph]].
- [122] G. Aad *et al.* [ATLAS Collaboration], JHEP **1509**, 108 (2015) [arXiv:1506.01291 [hep-ex]].
- [123] P. Achard *et al.* [L3 Collaboration], Phys. Lett. B **517**, 75 (2001) [hep-ex/0107015].
- [124] A. M. Sirunyan *et al.* [CMS Collaboration], Phys. Rev. D **100**, no. 5, 052003 (2019) [arXiv:1905.10853 [hep-ex]].
- [125] A. M. Sirunyan *et al.* [CMS], JHEP **07**, 142 (2019) doi:10.1007/JHEP07(2019)142 [arXiv:1903.04560 [hep-ex]].
- [126] CMS Collaboration [CMS Collaboration], CMS-PAS-EXO-18-005.
- [127] A. Buckley, J. M. Butterworth, L. Corpe, D. Huang and P. Sun, SciPost Phys. **9**, no.5, 069 (2020) doi:10.21468/SciPostPhys.9.5.069 [arXiv:2006.07172 [hep-ph]].
- [128] G. Abbiendi *et al.* [ALEPH, DELPHI, L3, OPAL and LEP], Eur. Phys. J. C **73**, 2463 (2013) doi:10.1140/epjc/s10052-013-2463-1 [arXiv:1301.6065 [hep-ex]].
- [129] G. Aad *et al.* [ATLAS], Eur. Phys. J. C **73**, no.6, 2465 (2013) doi:10.1140/epjc/s10052-013-2465-z [arXiv:1302.3694 [hep-ex]].
- [130] M. Aaboud *et al.* [ATLAS], JHEP **11**, 085 (2018) doi:10.1007/JHEP11(2018)085 [arXiv:1808.03599 [hep-ex]].
- [131] A. M. Sirunyan *et al.* [CMS], JHEP **07**, 142 (2019) doi:10.1007/JHEP07(2019)142 [arXiv:1903.04560 [hep-ex]].

- [132] T. Ma, B. Zhang and G. Cacciapaglia, Phys. Rev. D **89**, no. 9, 093022 (2014) [arXiv:1404.2375 [hep-ph]].
- [133] Y. Yu, C. X. Yue and S. Yang, Phys. Rev. D **91**, no. 9, 093003 (2015) [arXiv:1502.02801 [hep-ph]].
- [134] N. Kumar and S. P. Martin, Phys. Rev. D **92**, no. 11, 115018 (2015) [arXiv:1510.03456 [hep-ph]].
- [135] A. Alloul, N. D. Christensen, C. Degrande, C. Duhr, and B. Fuks, *FeynRules 2.0 - A complete toolbox for tree-level phenomenology*, *Comput. Phys. Commun.* **185** (2014) 2250–2300, [arXiv:1310.1921].
- [136] N. D. Christensen and C. Duhr, *FeynRules - Feynman rules made easy*, *Comput. Phys. Commun.* **180** (2009) 1614–1641, [arXiv:0806.4194].
- [137] J. Alwall, R. Frederix, S. Frixione, V. Hirschi, F. Maltoni, O. Mattelaer, H. S. Shao, T. Stelzer, P. Torrielli, and M. Zaro, *The automated computation of tree-level and next-to-leading order differential cross sections, and their matching to parton shower simulations*, *JHEP* **07** (2014) 079, [arXiv:1405.0301].
- [138] R. D. Ball et al., *Parton distributions with LHC data*, *Nucl. Phys.* **B867** (2013) 244–289, [arXiv:1207.1303].
- [139] T. Sjostrand, S. Mrenna, and P. Z. Skands, *PYTHIA 6.4 Physics and Manual*, *JHEP* **05** (2006) 026, [hep-ph/0603175].
- [140] **DELPHES 3** Collaboration, J. de Favereau, C. Delaere, P. Demin, A. Giammanco, V. Lemaître, A. Mertens, and M. Selvaggi, *DELPHES 3, A modular framework for fast simulation of a generic collider experiment*, *JHEP* **02** (2014) 057, [arXiv:1307.6346].
- [141] A. M. Sirunyan et al. [CMS Collaboration], Phys. Lett. B **782**, 440 (2018)